

Effects of Ligand Substituents (F for H; OR for R) on Mesogenic Properties of M(Salen) Derivatives (M = Cu, Ni, VO). New Fluoro-Substituted Complexes and Crystal Structure of the Mesogen Ni(5-hexylSalen)

Antony B. Blake,^{1a} John R. Chipperfield,^{*,1a} Wasif Hussain,^{1a} Reinhard Paschke,^{1b} and Ekkehard Sinn^{*,†,1a}

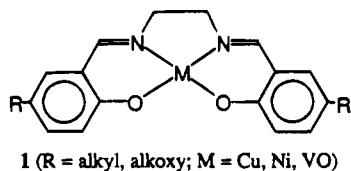
School of Chemistry, University of Hull, Kingston upon Hull HU6 7RX, U.K.

Received June 23, 1994[⊗]

The preparation of new metallomesogens containing fluoro-substituted bis(salicylaldehyde) ethylenediimine (Salen) ligands is reported for the complexes of copper(II), nickel(II), and oxovanadium(IV), in which substitution for individual atoms is shown to have a dramatic effect on packing and mesogenic properties. In other mesogens, fluoro substitution reduces melting points or extends the mesogenic range, or both. By contrast, in the title compounds the melting points are lowered by up to 50 °C, while the mesogenicity is eliminated or drastically reduced in range by fluorination, presumed to exert its influence through the dipolar effect. When the alkoxy O atom in Ni(5-(hexyloxy)Salen) is replaced with CH₂, the structure changes dramatically from roughly planar to an irregular S-shape, but mesogenic properties are retained. The crystal structure of (5-*n*-hexylSalen)Ni shows it to be an S-shaped molecule with especially dramatic bending at the *n*-hexyl chains from their phenyl rings (58, 85°). Crystal data: C₂₈H₃₈N₂O₂Ni, space group *P* $\bar{1}$, *a* = 12.640(2) Å, *b* = 16.872(2) Å, *c* = 6.650(2) Å, α = 98.54(3)°, β = 92.89(3)°, γ = 71.43(1)°, *Z* = 2, *R* = 5.44%, *R_w* = 5.96% for 1612 observed unique reflections.

Introduction

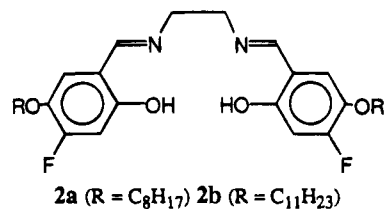
We have reported metallomesogens based on copper and nickel complexes of alkyl- and alkoxy-substituted Salen, **1**,^{2–4} and the crystal structures of two parent molecules in this series



Ni(Salen-OC₆)·H₂O (**1**; M = Ni; R = -OC₆H₁₃; hydrogen-bonded hydrate)² and Cu(Salen-OC₆)·CHCl₃ (**1**; M = Cu; R = -OC₆H₁₃; hydrogen-bonded chloroform solvate).⁴ Certain of the alkyl-substituted nickel complexes (**1**; M = Ni; R = C₆H₁₃, C₁₂H₂₅) have shown an S_E ⇌ S_A phase transition accompanying a dimer ⇌ monomer transition.⁵ A study of oxovanadium(IV) complexes of the ligands has also been made.⁶

These metallomesogens have high melting points, and synthesis of metallomesogens with low melting points is a pressing objective before their properties can be exploited in devices. Experience with organic mesogens has shown that aromatic fluoro substituents can often bring about reduction in

melting points,^{7–11} and it has also been shown that introduction of fluoro groups into metallomesogens, although not necessarily lowering melting points, does significantly alter phase behaviour.^{12,13} Consequently, we have synthesized new fluoro-substituted salicylaldehyde chelates **2a** and **2b** and their metal



complexes (Table 1) with oxovanadium(IV) (**3a**, **3b**), copper (**4a**, **4b**), and nickel (**5a**, **5b**). It is notoriously difficult to grow single crystals of such metallomesogens, but we have now managed to determine the structure of a single crystal of complex **1** (M = Ni; R = -C₆H₁₃).

Experimental Section

Synthesis of Ligands. (a) 4-Fluoro-5-(octyloxy)salicylaldehyde.

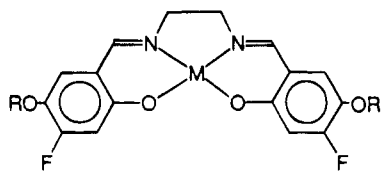
The hydroxy group of 2-fluoro-4-bromophenol was converted to alkoxy by treatment with appropriate bromoalkane in alkaline (KOH) DMF. The bromo group was converted to hydroxyl by the method of Kidwell *et al.*¹⁴ A formyl group was introduced by the paraformaldehyde/tin

[†] Fax: 011-44-482-46-6410. E-mail: e.sinn@chem.hull.ac.uk.

[⊗] Abstract published in *Advance ACS Abstracts*, February 1, 1995.

- (1) (a) University of Hull. (b) Institut für Anorganische Chemie, Martin-Luther Universität, Halle, Germany.
- (2) Paschke, R.; Balkow, D.; Baumeister, U.; Hartung, H.; Chipperfield, J. R.; Blake, A. B.; Nelson, P. G.; Gray, G. W. *Mol. Cryst. Liq. Cryst.* **1990**, *188*, 105.
- (3) Paschke, R.; Zschke, H.; Mädecke, A.; Chipperfield, J. R.; Blake, A. B.; Nelson, P. G.; Gray, G. W. *Mol. Cryst. Liq. Cryst. Lett.* **1988**, *6*, 81.
- (4) Paschke, R.; Sinn, E. Work in progress.
- (5) Ohta, K.; Morizumi, Y.; Fujimoto, T.; Yamamoto, I. *Mol. Cryst. Liq. Cryst.* **1992**, *214*, 161.
- (6) Serrette, A.; Carrol, P. J.; Swager, T. M. *J. Am. Chem. Soc.* **1992**, *114*, 1887.

- (7) Osman, M. A. *Mol. Cryst. Liq. Cryst.* **1885**, *128*, 45.
- (8) Coates, D. *Liq. Cryst.* **1987**, 423.
- (9) Gray, G. W.; Hird, M.; Lacey, D.; Toyne, K. J. *J. Chem. Soc., Perkin Trans. 2* **1989**, 2041.
- (10) Nestor, G.; Gray, G. W.; Lacey, D.; Toyne, K. J. *Liq. Cryst.* **1990**, *7*, 669.
- (11) Gray, G. W.; Hird, M.; Toyne, K. J. *Mol. Cryst. Liq. Cryst.* **1991**, *204*, 43.
- (12) Thompson, N. J.; Goodby, J. W.; Toyne, K. J. *Mol. Cryst. Liq. Cryst.* **1992**, *214*, 81.
- (13) Bruce, D. W.; Dhillon, R.; Dunmur, D. A.; Maitlis, P. M. *J. Mater. Chem.* **1992**, *2*, 65.
- (14) Kidwell, R. L.; Murphy, M.; Darling, S. D. *Org. Synth.* **1969**, *49*, 90.

Table 1. Phase Properties of Complexes

complex	M	R	phases (transition temperature/°C) [data for unfluorinated analogues in brackets] ^c
3a	VO	C ₈ H ₁₇	K 198 I [Sc ₂ 62 Sc ₁ 179 S _A 198 I]* ^a
3b	VO	C ₁₁ H ₂₃	K 186 (S _A 165) ^b [Sc ₂ 65 Sc ₁ 157 S _A 210 I]* ^c
4a	Cu	C ₈ H ₁₇	K 254–255 I [K 248 S _A 273 I] ^a
4b	Cu	C ₁₁ H ₂₃	K 240 I [K 253 (S _A 252) I]* ^a
5a	Ni	C ₈ H ₁₇	K 250 (S _A 246) I [K 61 S ₁ 186 S _A 300 I] ^a
5b	Ni	C ₁₁ H ₂₃	K 226 S _A 227 I [K ~ 175 S _A ~ 300 I] ^d

^a Reference 2. ^b On cooling, majority of I phase crystallizes at ~168 °C, but remainder shows S_A phase at 165 °C. ^c Interpolated from data in ref. 6. ^d Extrapolation from data in ref. 2. *: on cooling. K = crystalline; S_A = smectic A; I = isotropic; parentheses denote monotropic phase.

tetrachloride method of Casiraghi *et al.*¹⁵ Before extraction with ether, the product-containing solution was saturated with NaCl. After column chromatography on silica (30–70 mesh), eluting with 1:4 CH₂Cl₂/hexane, and removal of the solvent from the middle fraction, a light-brown liquid was obtained which yielded white crystals of 4-fluoro-5-(octyloxy)salicylaldehyde after refrigeration (yield 19.4%). δ_{H} (CDCl₃; SiMe₄): 0.75–1.95 (15 H, C₇H₁₅), 4.0 t (2 H, OCH₂), 6.75 d, 7.1 d (2 H, C₆H₂), 9.85 (1 H, CHO), 11.07 s (1 H, OH). At δ 6.75 ³J_{H-F} = 12.0 Hz; at δ 7.1 ⁴J_{H-F} = 9.0 Hz.

(b) **4-Fluoro-5-(undecyloxy)salicylaldehyde** was prepared similarly (yield 23%). δ_{H} (CDCl₃; SiMe₄): 0.65–1.95 (21 H, C₁₀H₂₁), 3.95 t (2 H, OCH₂), 6.70 d, 7.1 d (2 H, C₆H₂), 9.80 s (1 H, CHO), 11.05 (1 H, OH). Melting points could not be obtained for the above two compounds, as these products became oily at room temperature.

(c) **2,2'-(1,2-Ethanediybis(nitrilomethylidene))bis[5-fluoro-4-(octyloxy)phenol]**, **2a**, was prepared by stirring (4 h) the substituted salicylaldehyde and 1,2-diaminoethane in the correct molar ratio in dichloromethane over molecular sieve 4A. Removal of solvent and recrystallization from dichloromethane/petroleum ether (bp 40–60 °C) gave a yellow microcrystalline solid (yield 82%); mp 155 °C. Anal. Calcd for C₃₂H₄₆F₂N₂O₄: C, 68.55; H, 8.27; N, 4.99. Found: C, 68.0; H, 8.02; N, 4.74. δ_{H} (CD₂Cl₂; SiMe₄): 0.8–1.95 (30 H, 2 C₇H₁₅), 3.95 br t (8 H, 2 NCH₂, 2 OCH₂), 6.85 d, 6.65 d (4 H, 2 C₆H₂), 8.25 s (2 H, 2 CH=N), 13.25 br s (2H, 2 OH). At δ 6.65 ³J_{H-F} = 12.5 Hz; at δ 6.85 ⁴J_{H-F} = 9.0 Hz. MS (EI): M⁺ 560.

(d) **2,2'-(1,2-Ethanediybis(nitrilomethylidene))bis[5-fluoro-4-(undecyloxy)phenol]**, **2b**, was prepared by stirring the substituted salicylaldehyde and 1,2-diaminoethane in methanol for 1 h. The bright yellow product was filtered off, washed with petroleum ether (bp 40–60 °C), dried under vacuum at 40 °C, and recrystallized from CH₂Cl₂ (yield 54.8%); mp 145 °C. (Found C, 70.4; H, 9.00; N, 4.38. C₃₈H₅₈F₂N₂O₄ requires C, 70.77; H, 9.06; N, 4.34%) δ_{H} (CDCl₃; SiMe₄) 0.8–1.9 (42H, 2 C₁₀H₂₁), 3.9 s br (8 H, 2 NCH₂, 2 OCH₂), 6.80 d, 6.65 d (4 H, 2 C₆H₂), 8.20 (2 H, 2 CH=N), 13.20 s br (2 H, 2 OH). At δ 6.65 ³J_{H-F} = 12.4 Hz; at δ 6.80 ⁴J_{H-F} = 9.0 Hz. MS (EI) M⁺ 644.

Preparation of Complexes. (a) **(4-Fluoro-5-(octyloxy)Salen)oxovanadium(IV)**, **3a**. To a suspension of **2a** (0.12 g, 0.22 mmol) in ethanol (15 mL) was added an aqueous solution (1 mL) containing

hydrated vanadyl sulfate (0.05 g, 0.24 mmol) and sodium acetate (0.053 g, 0.65 mmol). The mixture was stirred at 60 °C for 3 h and cooled, and the crude product was filtered off. After washing with water and then ethanol, the product was twice recrystallized from CH₂Cl₂/MeOH to yield 0.05 g (37%) of a microcrystalline green solid. Anal. Calcd for C₃₂H₄₄F₂N₂O₅V: C, 61.43; H, 7.08; N, 4.47. Found: C, 61.2; H, 7.12; N, 4.48.

(b) **(4-Fluoro-5-(undecyloxy)Salen)oxovanadium(IV)**, **3b**, was prepared similarly as bright green microcrystals (yield 50.1%). Anal. Calcd for C₃₈H₅₆F₂N₂O₅V: C, 64.3; H, 7.95; N, 3.94. Found: C, 64.1; H, 7.99; N, 3.93.

(c) **(4-Fluoro-5-(octyloxy)Salen)copper(II)**, **4a**. To a solution of **2a** (0.2 g, 0.36 mmol) in ethanol (20 mL) was added an aqueous solution (1 mL) of copper acetate (0.079 g, 0.4 mmol) and sodium acetate (0.1 g, 1.23 mmol), and the mixture was stirred at 80 °C for 4 h. The solid formed was filtered off at room temperature, washed with water and then ethanol, and recrystallized from CH₂Cl₂/MeOH to give 0.13 g (59%) of a green microcrystalline solid. Anal. Calcd for C₃₂H₄₄-CuF₂N₂O₄: C, 61.76; H, 7.12; N, 4.50. Found: C, 61.5; H, 6.98; N, 4.32.

(d) **(4-Fluoro-5-(octyloxy)Salen)nickel(II)**, **4b**, was prepared similarly (yield 65.4%) but could not be recrystallized from CH₂Cl₂/MeOH. Anal. Calcd for C₃₈H₅₆CuF₂N₂O₄: C, 64.61; H, 7.99; N, 3.96. Found: C, 64.3; H, 8.07; N, 4.02.

(e) **(4-Fluoro-5-(undecyloxy)Salen)nickel(II)**, **5a**, was prepared similarly from **2a**, hydrated nickel acetate, and sodium acetate. The crude product was dissolved in CH₂Cl₂, and the solution was filtered. The product was reprecipitated with MeOH and recrystallized twice from CH₂Cl₂/MeOH to give reddish-brown microcrystals (yield 39.3%). Anal. Calcd for C₃₂H₄₄F₂N₂NiO₄·H₂O: C, 60.5; H, 7.29; N, 4.40. Found: C, 60.4; H, 7.27; N, 4.42. δ_{H} (CDCl₃; SiMe₄): 1.55 s (H₂O of crystallization), 0.75–1.9 multiplet (30 H, 2 C₇H₁₅), 3.45 (4 H, 2 CH₂), 3.85 t (4 H, 2 OCH₂), 6.7 d, 6.45 d (4 H, 2 C₆H₂), 7.2 s (2 H, 2 CH=N). At δ 6.7 ³J_{H-F} = 14.0 Hz; at δ 6.45 ⁴J_{H-F} = 10.0 Hz.

(f) **5b** was prepared similarly from **2b** and was recrystallized from CHCl₃/hexane to give a yellow solid (yield 34.8%). Anal. Calcd for C₃₈H₅₆F₂N₂NiO₄·H₂O: C, 63.4; H, 8.12; N, 3.89. Found: C, 63.4; H, 7.92; N, 3.85. δ_{H} (CDCl₃; SiMe₄): 1.57 s (H₂O of crystallization), 0.75–1.9 multiplet (42 H, 2 C₁₀H₂₁), 3.42 (4 H, 2 CH₂), 3.85 t (4 H, 2 OCH₂), 6.72 d, 6.45 d (4 H, 2 C₆H₂), 7.17 s (2 H, 2 CH=N). At δ 6.72 ³J_{H-F} = 14.0 Hz; at δ 6.45 ⁴J_{H-F} = 10.0 Hz.

For all products IR spectra were consistent with structures proposed.

Phase Studies. The phase behaviour of the complexes was examined by using an Olympus BH2 polarizing microscope, in conjunction with a Mettler FP5 hot stage and controller, and also by DSC studies.

Crystal Structure Determination of (5-n-hexylSalen)Ni. Orange-red lath-shaped crystals, prepared as previously described,² were grown by slow evaporation of a solution in toluene and submitted to the SERC X-ray Crystallography Service for diffraction data collection on an Enraf-Nonius CAD4 four-circle diffractometer.

Computations were carried out using the data with $F_o^2 > 3\sigma(F_o^2)$, where $\sigma(F_o^2)$ was estimated from counting statistics.¹⁶ Corrections for Lorentz and polarization effects and for absorption¹⁷ were applied. The position of the metal atom was determined from a Patterson map. Other atoms were located from Fourier difference syntheses. The refinement and final full-matrix least-squares refinement, based on F , was carried out using the TEXRAY program set.¹⁸ The function minimized was $\sum w(|F_o| - |F_c|)^2$ where $w = 4F_o^2/\sigma^2(F_o^2)$, $\sigma^2(F_o^2) = [S^2(C + R^2B) + 0.03F_o^2]/(\text{Lp})^2$, S = scan rate, C = total integrated peak count, R = ratio of scan time to background counting time, B = total background count, and Lp = Lorentz–polarization factor. Atomic scattering factors for non-hydrogen atoms were taken from Cromer and Waber,¹⁹ and those for hydrogen, from Stewart and Davidson.²⁰ The effects of

(16) Corfield, P. W. R.; Doedens, R. J.; Ibers, J. A. *Inorg. Chem.* **1967**, *6*, 197.

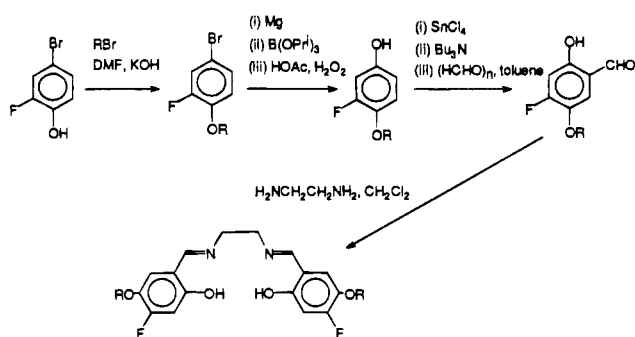
(17) Walker, N.; Stuart, D. *Acta Crystallogr.* **1983**, *A39*, 158.

(18) *TEXRAY Structure Analysis Package*; Molecular Structure Corp.: Houston, TX, 1985.

(19) Cromer, D. T.; Waber, J. T. *Acta Crystallogr.* **1965**, *18*, 511.

(20) Stewart, R. F.; Davidson, E. R. *J. Chem. Phys.* **1965**, *45*, 3175.

(15) Casiraghi, G.; Casnati, G.; Puglia, G.; Sartori, G.; Terenghi G. *J. Chem. Soc., Perkin Trans. 1* **1980**, 1862.

Scheme 1. Synthesis of Fluoro-Substituted Salicylalimine Ligands

anomalous dispersion were included using values for $\Delta f'$ and $\Delta f''$ from Cromer.²¹ The structure was refined with anisotropic thermal parameters for all non-H atoms. The successful refinement confirmed the choice of the centric space group.

Results and Discussion

Fluoro-Substituted Complexes. Synthesis of ligands containing fluoro-substituted aromatic rings is best achieved by starting with the fluoro substituent already in place. Our synthetic strategy is shown in Scheme 1. The most difficult step is the introduction of the $-CHO$ group onto a 3-fluoro-4-alkoxyphenol. Although yields of the tin tetrachloride/paraformaldehyde route were low, no better route was found.

The phase properties of the oxovanadium(IV), copper, and nickel complexes of **2a** and **2b** are compared with those of the corresponding unfluorinated complexes in Table 1. It can be seen that introduction of a fluorine atom into the 4-position completely suppresses the liquid crystal phase in three cases (**3a**, **4a**, **4b**). In two cases (**3b** and **5a**), S_A phases in the unsubstituted complexes are replaced by monotropic S_A phases in the fluorinated derivatives, with a substantial increase in melting temperature in each case. In compound **5b**, a narrow S_A phase survives, but the melting point is again relatively high. For each fluorinated complex except **3a** the melting or clearing temperature is lower (by up to 50 °C) than the clearing temperature of its unfluorinated analog. The effect on phase behaviour is even more significant than the dramatic effect on the temperature lowering. The F atoms are too small to produce a significant steric effect. Instead, the electrostatic effect of interchanging C-H and C-F in the 4-position must be responsible for the change in intermolecular forces that lead to the stark change we observe in phase behavior. It is clear that in these Ni(Salen) derivatives, isotropic (I) phases are achieved at substantially lower temperatures by replacing the 4-H with an F atom, but to widen the mesogenic range, we must go in the opposite direction.

In the terphenyl series of liquid crystal materials, the most impressive lowering of melting and clearing temperatures by fluorination is seen in unsymmetrical molecules.^{9,11} Complexes of unsymmetrical salicylaldimines with one fluorosubstituted and one unsubstituted ring might be expected to show mesophases at reduced temperatures, and we intend to investigate this type of complex.

No structural data are available for the fluoro complexes, as no suitable crystals have yet been isolated. The powder XRD pattern for the 4-F derivative of Cu(5-(octyloxy)Salen) shows similarities to that of the 4-H analog, but the patterns are different enough to indicate that the two forms are not truly isomorphous. Given the different mesogenic properties ob-

Table 2. Crystal Data, Intensity Collection Parameters, and Details of Refinement for (5-*n*-hexylSalen)Ni

formula	C ₂₈ H ₃₈ N ₂ O ₂ Ni
molar mass	493.3 g mol ⁻¹
<i>a</i> , <i>b</i> , <i>c</i>	12.640(2), 16.872(3), 6.650(1) Å
α , β , γ	98.54(3), 92.89(3), 71.43(1)°
<i>V</i>	1329.4 Å ³
system, space group	triclinic, $P\bar{1}$
<i>Z</i> , <i>D</i> _c	2, 1.232 g cm ⁻³
<i>F</i> (000)	528
radiation, wavelength	Cu K α , 1.5418 Å
linear abs coeff μ	12.45 cm ⁻¹
θ : min, max	3.0, 60.0°
temp	293 K
no. of reflns measd	5280
no. of unique reflns	3949
no. of reflns obsd [$F_o > 3\sigma(F_o)$]	1612
no. of params	298
abs corr	DIFABS
weighting scheme	$w = [\sigma(F_o) + 0.01F_o^2]^{-1}$
final <i>R</i> , <i>R</i> _w ^a	0.0544, 0.0596

$$^a R = \sum ||F_o| - |F_c|| / \sum |F_o|; R_w = [(\sum w(|F_o| - |F_c|)^2 / \sum w F_o^2)]^{1/2}.$$

Table 3. Positional Parameters and *B*(eq) Values for (5-*n*-hexylSalen)Ni

atom	<i>x</i>	<i>y</i>	<i>z</i>	<i>B</i> (eq), Å ²
Ni	-0.0114(1)	-0.01739(9)	0.2426(2)	6.66(9)
O(1)	-0.1431(5)	-0.0420(3)	0.2417(7)	5.1(4)
O(2)	0.0506(5)	-0.1344(3)	0.1810(7)	5.1(4)
N(1)	-0.0762(7)	0.0977(4)	0.3076(9)	4.5(5)
N(2)	0.1229(6)	0.0034(5)	0.2400(9)	4.5(5)
C(1a)	-0.266(1)	0.0991(8)	0.300(1)	5.2(8)
C(2a)	-0.242(1)	0.0111(8)	0.258(1)	5.4(8)
C(3a)	-0.338(1)	-0.0157(6)	0.231(1)	6.5(7)
C(4a)	-0.444(1)	0.038(1)	0.247(1)	7.8(9)
C(5a)	-0.468(1)	0.123(1)	0.287(1)	7.3(8)
C(6a)	-0.377(1)	0.1527(6)	0.317(1)	6.6(8)
C(7a)	-0.180(1)	0.1362(5)	0.327(1)	5.4(7)
C(8a)	0.0040(8)	0.1437(5)	0.346(1)	6.1(6)
C(9a)	-0.5886(9)	0.1809(7)	0.301(2)	9.5(8)
C(10a)	-0.6369(9)	0.2052(6)	0.508(2)	9.3(8)
C(11a)	-0.7530(8)	0.2629(6)	0.529(2)	9.2(8)
C(12a)	-0.795(1)	0.287(1)	0.744(3)	17(1)
C(13a)	-0.899(1)	0.341(1)	0.780(2)	17(2)
C(14a)	-0.933(1)	0.362(1)	0.992(3)	23(2)
C(1b)	0.2425(9)	-0.1415(7)	0.176(1)	4.4(7)
C(2b)	0.1557(9)	-0.1766(7)	0.162(1)	5.2(7)
C(3b)	0.1839(8)	-0.2653(7)	0.127(1)	6.8(7)
C(4b)	0.293(1)	-0.3133(5)	0.101(1)	7.4(8)
C(5b)	0.3795(8)	-0.2793(7)	0.113(1)	6.0(7)
C(6b)	0.3524(9)	-0.1944(7)	0.148(1)	5.6(7)
C(7b)	0.2190(9)	-0.0533(7)	0.212(1)	4.9(7)
C(8b)	0.1123(7)	0.0924(6)	0.259(1)	6.2(7)
C(9b)	0.4993(8)	-0.3385(6)	0.073(2)	8.2(8)
C(10b)	0.5202(8)	-0.3899(6)	-0.133(2)	7.7(7)
C(11b)	0.6416(8)	-0.4358(6)	-0.181(2)	8.4(8)
C(12b)	0.666(1)	-0.4878(7)	-0.380(2)	9.9(9)
C(13b)	0.788(1)	-0.5301(8)	-0.424(2)	12(1)
C(14b)	0.809(1)	-0.582(1)	-0.615(2)	19(1)

served in the fluoro derivatives studied, it is not unreasonable that the fluoro substitution produces some differences in the crystal structures.

A most dramatic substituent effect emerges from comparing Ni(5-(hexyloxy)Salen) and Ni(5-hexylSalen), which corresponds to insertion of O between the phenyl ring and the first CH₂ and leads to the very different molecular shapes discussed below. However, in this case the mesogenic properties change far less than might be predicted from so great a structural change.

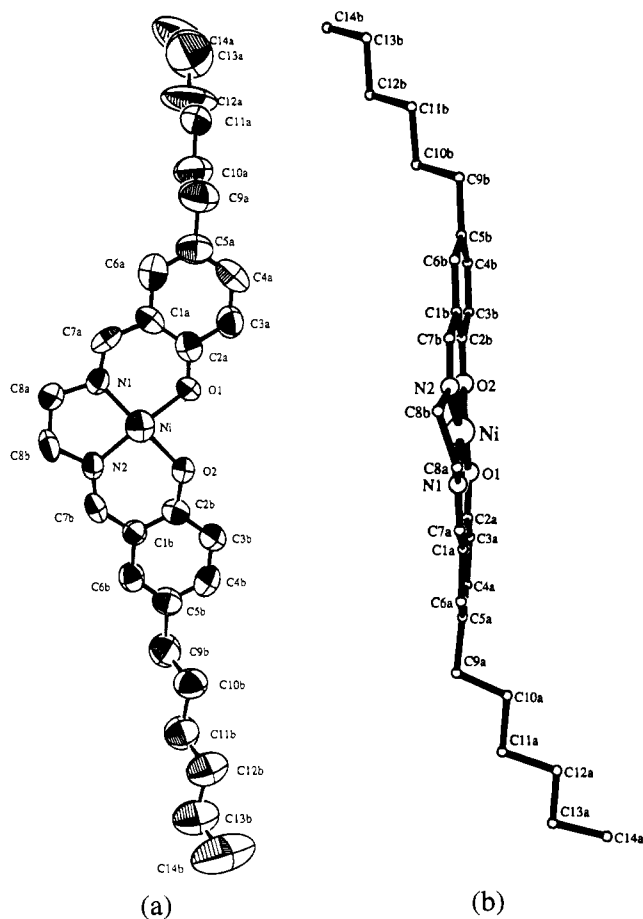
Structure of Ni(5-hexylSalen) (1; M = Ni; R = C₆H₁₃). Crystal data and details of the data collection procedure are listed in Table 2. Table 3 lists atomic and thermal parameters, and Table 4 gives selected interatomic distances and angles. ORTEP

(21) Cromer, D. T. *Acta Crystallogr.* **1965**, *18*, 17.

Table 4. Selected Bond Lengths (Å), Bond Angles (deg) and Nonbonded Distances (Å) for (5-*n*-hexylSalen)Ni

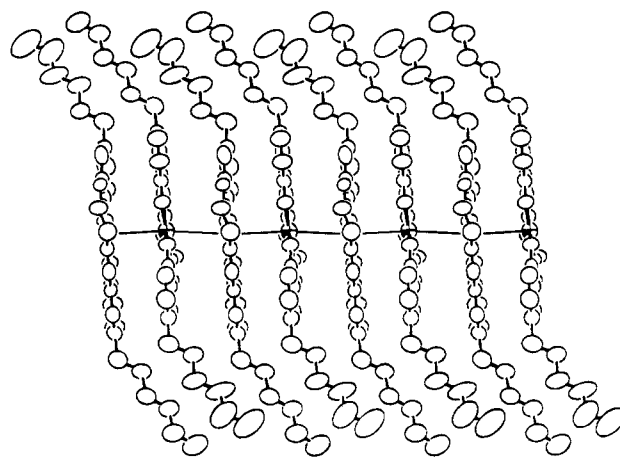
Bond Lengths			
Ni—O(1)	1.840(5)	Ni—O(2)	1.867(6)
Ni—N(1)	1.845(7)	Ni—N(2)	1.840(7)
O(1)—C(2a)	1.29(1)	O(2)—C(2b)	1.294(9)
N(1)—C(7a)	1.27(1)	N(2)—C(7b)	1.29(1)
N(1)—C(8a)	1.45(1)	N(2)—C(8b)	1.45(1)
C(1a)—C(2a)	1.40(1)	C(1b)—C(2b)	1.40(1)
C(1a)—C(7a)	1.41(1)	C(1b)—C(7b)	1.41(1)
Bond Angles			
O(1)—Ni—O(2)	83.3(3)	N(1)—Ni—N(2)	86.9(3)
O(1)—Ni—N(1)	95.1(3)	O(2)—Ni—N(2)	94.7(3)
O(1)—Ni—N(2)	178.0(4)	O(2)—Ni—N(1)	178.2(3)
Ni—O(1)—C(2a)	126.9(6)	Ni—O(2)—C(2b)	126.5(6)
Ni—N(1)—C(7a)	125.6(7)	Ni—N(2)—C(7b)	125.4(6)
Ni—N(1)—C(8a)	113.7(6)	Ni—N(2)—C(8b)	113.9(6)
N(1)—C(7a)—C(1a)	126(1)	N(2)—C(7b)—C(1b)	127.7(9)
N(1)—C(8a)—C(8b)	110.4(7)	N(2)—C(8b)—C(8a)	110.2(7)
C(7a)—N(1)—C(8a)	120.7(8)	C(7b)—N(2)—C(8b)	120.6(7)
C(2a)—C(1a)—C(7a)	121(1)	C(2b)—C(1b)—C(7b)	120(1)
Nonbonded Distances			
Ni—Ni ^a	3.406(4)	Ni—Ni ^b	3.400(4)
Ni—N(2) ^a	3.449(7)	Ni—O(2) ^a	3.991(6)
Ni—N(1) ^b	3.453(7)	Ni—O(1) ^b	4.016(6)

^a Atom at $-x, -y, -z$. ^b Atom at $-x, -y, 1 - z$.

**Figure 1.** Top (a) and side (b) views of (5-hexylSalen)Ni showing the severe bending in the molecule.

views²² of the molecule are shown in Figure 1. Figure 2 shows the stacking in a slightly zigzag column parallel with the *c* axis.

The crystal structures of the parent complex Ni(Salen) and a number of its complexes with large cations have been reported.^{23,24} The only previously reported structure determination

**Figure 2.** Stacking along the *c* axis.**Table 5.** Distances (Å) and Angles (deg) around the Nickel Atom in (5-R-Salen)Ni

	R = H	R = C ₆ H ₁₃ O	R = C ₆ H ₁₃
Ni—O(1)	1.850(2)	1.849(3)	1.840(5)
Ni—O(2)	1.855(2)	1.851(3)	1.867(6)
Ni—N(1)	1.853(2)	1.852(3)	1.845(7)
Ni—N(2)	1.843(2)	1.838(3)	1.840(7)
Ni—Ni'	3.201(2)	6.633(1)	3.400, 3.406(4)
O(1)—Ni—O(2)	85.6(1)	85.3(2)	83.3(3)
N(1)—Ni—N(2)	86.3(1)	86.0(2)	86.9(3)
O(1)—Ni—N(1)	93.9(1)	94.2(2)	95.1(3)
O(2)—Ni—N(2)	94.3(1)	94.7(2)	94.7(3)
reference	23	2	this work

of a substituted Salen nickel complex is that of (5-(hexyloxy)-Salen)Ni·H₂O.² In view of the different mesophase properties of the hexyl and hexyloxy compounds, it is of interest to compare the molecular structures and packing arrangements of these and with those of the parent molecule. Some relevant dimensions are collected in Table 5, from which it can be seen that there are no significant differences in bond lengths and angles around the nickel atoms between the hexyl and hexyloxy compounds or between these and the unsubstituted complex. There are, however, significant differences in overall shapes and packing arrangements among the three compounds.

Molecules of Ni(Salen) pack as centrosymmetric "face-to-face" dimers separated by 3.08 Å, with the component molecules only very slightly displaced parallel to their long axis, resulting in a Ni···Ni distance of 3.20 Å, significantly shorter than the shortest intermolecular Ni···O distance of 3.36 Å.²³

In Ni(5-hexyloxy)Salen·H₂O, the molecules also occur as centrosymmetric dimers, but now with a much greater displacement so that the Ni atoms in the component molecules are 6.87 Å from each other.² The shortest intermolecular contacts of the Ni atoms are 3.75 and 3.97 Å to alkoxy O atoms and 3.81 Å to a 5-carbon atom of neighboring dimers. Although such Ni···O distances rule out any significant intermolecular bonding, it is possible that weak electrostatic interactions may favor this displacement. The water molecule is not coordinated but lies within hydrogen-bonding distance of a ligand oxygen atom. The alkoxy groups are extended, they lie approximately in the Salen

(22) Johnson, C. K. ORTEPII. Report ORNL-5138; Oak Ridge National Laboratory: Oak Ridge, TN, 1976.

(23) Manfredotti, A. G.; Guastini, C. *Acta Crystallogr.* **1983**, *39C*, 863. Skol'nikova, L. M.; Jumal, E. M.; Sugam, E. A.; Voblikova, V. A. *J. Struct. Chem. USSR (Engl. Transl.)* **1970**, *11*, 819.

(24) Giacomelli, A.; Floriani, C.; Perego, G. *J. Chem. Soc., Chem. Commun.* **1982**, 650. Pahor, N. B.; Calligaris, M.; Delise, P.; Nardin, G.; Randaccio, L.; Zotti, E.; Fachinetti, G.; Floriani, C. *J. Chem. Soc., Dalton Trans.* **1976**, 2310.

plane, and all point roughly along the same direction in the crystal. It is this feature that makes the most stark contrast with the geometry in (5-hexylSalen)Ni.

In (5-hexylSalen)Ni, the molecules are again face to face, as in (Salen)Ni, but now almost uniformly stacked along the [001] direction, as shown in Figure 2, with relatively short Ni···Ni distances of alternatively 3.400 and 3.406 Å. The Ni atoms are slightly offset from the *c* axis, giving a Ni···Ni'···Ni'' angle of 155.4°. The shortest distances of the Ni atom to ligand atoms of neighboring molecules are 3.45 Å to N atoms. The first coordination sphere is very flat, but the overall molecule is far from planar. Instead the molecule is markedly *S*-shaped, with half the ligand (fragment *a*) bending far more than the other (fragment *b*). The central approximately planar "rigid" central part of the molecule displays an *S*-bend which follows the much more dramatic *S*-bend of the alkyl chains. This is apparent from the detailed geometric relationship between the fragments. The metal atom deviates from the central N₂O₂ plane by only 0.005 Å. The angle made at Ni by the halves of the ligand, as measured by the two NiNO planes, is only 0.9°, a tiny bend toward the 90° required for tetrahedral. The OCCCN planes of the ligand are slightly displaced from the Ni (0.11 and 0.07 Å for fragments *a* and *b*, respectively) and are slightly bent in an *S* shape away from the N₂O₂ center (4.6° for *a* and 3.2 for *b*). The two phenyl rings bent further away, but again at relatively small angles, from the OCCCN planes (2.4 and 0.6° for *a* and *b*, respectively). The two C₆ chains are each remarkably planar (average deviations 0.020 and 0.011 Å in *a* and *b*, respectively); these planes bend sharply away from their phenyls (85.1° for *a* and 57.8° for *b*) and incline at 33.8° to each other. The molecules stack as centrosymmetrically related pairs (6). Although the alkyl chains point in significantly



different directions, the two rigid NiSalen fragments are parallel if we ignore the fact that they are not quite flat. Figure 2 shows this stacking as a zigzag column parallel with the *c* axis. The calculated density of the crystal is about 7% lower than that of the hexyloxy-substituted complex, and this may be related to the fact that the equivalent isotropic thermal vibration parameters are greater than those in the latter compound, especially those of the alkyl carbon atoms (B_{eq} 8–23, compared to 4–8 Å²).

The slightly different alternate Ni···Ni distances in the crystal fit in well with Ohta's observation that the S_E phase consists of dimers.⁵

It is of interest that the Ni···Ni distance here, 3.40 Å, is comparable with that found in many of the "stacked" glyoximates of nickel (3.19–3.60 Å²⁵). The latter typically show a longitudinally polarized solid–solid optical transition and semiconducting behaviour along the stacking axis which have been discussed in terms of extended metal–metal interactions.²⁶

Although understanding of the relationship between molecular structure and phase behaviour of metallomesogens is scarcely developed as yet, it is perhaps worth noting that both Ni(5-*n*-hexylSalen) and Ni(5-(*n*-hexyloxy)Salen) show three smectic phases; but the hexyl-substituted complex, whose molecules are stacked in the crystal with all of them similarly aligned, has a considerably lower melting temperature and a wider smectic phase range (K → S₁, S₁ → S₂, S₂ → S_A, and S_A → I at 84, 118, 245, and 310 °C, where the precise nature of the S₁ and S₂ phases has not yet been fully established)²⁷ than the hexyloxy analog (148, 229, 241, and 317 °C), in which the molecules are arranged in the crystal in a double-herringbone fashion in two distinct orientations.² Optical spectra as a function of temperature will show how well the solid state features are preserved in the mesophase and provide useful comparison between the complexes. Apparatus is being set up for such measurements.

Acknowledgment. We thank the SERC for financial support under Grant GR/G08620, Dr. A. Slaney and Mrs. J. Haley for assistance with optical microscopy and DSC measurements, and the SERC X-ray Crystallography Service for data collection.

Supplementary Material Available: Tables of positional and anisotropic thermal parameters, bond distances and angles, least-squares planes, and X-ray powder data comparing fluoro and non-fluoro complexes (11 pages). Ordering information is given on any current masthead page.

IC940732Q

- (25) Godycki, I. E.; Rundle, R. E. *Acta Crystallogr.* **1953**, *6*, 487. Banks, C. V.; Barnum, D. W. *J. Am. Chem. Soc.* **1958**, *80*, 3579, 4767.
- (26) Thomas, T. W.; Underhill, A. E. *Chem. Soc. Rev.* **1972**, *1*, 99. Anex, B. G. In *Extended Interactions between Metal Ions*; Interrante, L. V., Ed.; ACS Symposium Series; American Chemical Society: Washington, DC, 1974.
- (27) Disagreement between mesophase transition temperatures for (5-*n*-hexylSalen)Ni^{2.5} probably arises from the presence of different impurities and decomposition products and is under investigation.